ELSEVIER

Journal of Membrane Science 211 (2003) 1–11

journal of MEMBRANE SCIENCE

www.elsevier.com/locate/memsci

Fouling behaviour of polyethersulfone UF membranes made with different PVP

J. Marchese [a], M. Ponce [a], N.A. Ochoa [a], P. Prádanos [b], L. Palacio [b], A. Hernández [b,*]

[a] *Grupo de Desarrollo y Tecnología de Membranas, Laboratorio de Ciencias de Superficies y Medios Porosos, UNSL-CONICET, Chacabuco y Pedernera, 5700 San Luis, Argentina*

[b] *Group of Surfaces and Porous Materials (SMAP), Departmento de Termodinámica y Física Aplicada, Facultad de Ciencias, Universidad de Valladolid, 47071 Valladolid, Spain*

Received 25 February 2002; received in revised form 24 May 2002; accepted 27 May 2002

Abstract

Several polyethersulfone (PES) ultrafiltration membranes have been made with small quantities of polyvinyl-pyrrolidone (PVP) of different molecular weights to increase the permeability without a significant reduction in selectivity. The corresponding fouling mechanism and subsequent structural modifications have been analyzed when in contact with bovine serum albumin (BSA) and DL-histidine (DLH). It has been shown that according to the relative sizes of solute and pores of the membranes: BSA fouls the three membranes externally whereas DLH fouls them internally. Moreover, BSA fouls the non-PVP membranes faster than DLH fouls them slower, according to the action of hydrophobic and electrostatic forces acting at the working pH (4.9). The changes in structure, remaining after water rinsing, is quite similar for the three membranes and both the solutes, as obtained by a r etention test of adequate polyethylene glycols (PEGs).

Keywords: Ultrafiltration membranes; Fouling mechanisms; Pore size distributions; Retention tests; Solute–membrane interactions

1. Introduction

The main factors determining the membrane behaviour in a filtration process are the structure, the chemical composition and the operation conditions [1]. Structure, involving pore size distribution or pore density and the active layer thickness is the main factor in determining the flux and retention. However, these parameters are strongly influenced by the chemical composition of the material, which has a great influence on adsorption and fouling mechanisms in the surface and inside the pores, [2,3]. In the manufacture of membranes by phase inversion, it is common to add different substances, to control both structure and chemical interactions [4–10].

In a previous work [11], the effect of small quantities of polyvinyl-pyrrolidone (PVP) in the structure of a polyethersulfone (PES) membrane, made by phase inversion, was studied. The pore size distribution of membranes, with similar selectivities but different permeate flux, were shown to be very similar by AFM and permeation of polydispersed solutes (polyethylene glycols (PEGs)). The different hydraulic permeability obtained for these membranes with similar pore size distributions shows that they must have different porosities, tortuosities and/or thickness of the dense layer. Other possibility is the appearance of bigger macrovoids under the dense layer, decreasing

* Corresponding author. Tel.: +34-983-42-3134; fax: +34-983-42-3013.
E-mail address: membrana@termo.uva.es (A. Hernández).

0376-7388/02/$ – see front matter
PII: S0376-7388(02)00260-0

Nomenclature

A	membrane area (m^2)
B	constant of the Eq. (6) (Da)
c_0	feed concentration given as a volume fraction
c_m	membrane concentration in contact with the high-pressure interface given as a volume fraction
$c_{m,k}$	membrane concentration, given as a volume fraction, in contact with the high-pressure interface, for each molecular weight of a polydisperse mixture
c_p	permeate concentration given as a volume fraction
$c_{p,k}$	permeate concentration, given as a volume fraction, for each molecular weight of a polydisperse mixture
C	exponent of the Eq. (6)
C_{CB}	number of pores per surface unit blocked per unit of filtered volume (m^{-5})
C_{CF}	apparent specific resistance of the cake (m/kg)
C_S	volume deposited on the pore walls per unit of permeated volume (s/m)
d_p	pore diameter (m)
J_s	solute flux (m/s)
J_V	volumetric flux (m/s)
$J_V(t)$	volumetric flux at time t (m/s)
$J_{V,t}$	volumetric flux transmitted through the non-rejecting fraction of pores (m/s)
J_w	pure water flux (m/s)
$J_{w,t}$	pure water flux transmitted through the non-rejecting fraction of pores (m/s)
$J_{w,r}$	pure water flux transmitted through the rejecting fraction of pores (m/s)
J_{V0}	initial volumetric flux (m/s)
K	normalization constant in Eq. (6) (m^4)
K	kinetic constant in Eq. (10) (s^{-1})
K_{CB}	kinetic constant for complete blocking model (s^{-1})
K_{CF}	kinetic constant for cake filtration blocking model (s/m^2)
K_S	kinetic constant for standard blocking model (m^{-1})
M_w	molecular weight of the solute (Da)
N	cumulative pore density (m^{-2})
N_0	initial number of pores per surface unit (m^{-2})
N_T	total pore density (m^{-2})
Δp	the applied pressure (Pa)
r_0	the initial mean pore size (m)
R	true retention coefficient
$R[M_w(i)]$	Accumulate true retention coefficient for a polydisperse mixture of solutes defined in Eq. (7)
R_o	observed or apparent retention coefficient
t	time (s)
V	permeate volume (m^3)
V^*	permeate volume until time t per surface unit of membrane (m)

Greek letters

ℓ_0	membrane thickness (m)
ρ_C	the cake mass per unit of permeated volume (kg/m^3)
η	solution viscosity (kg/m s)
$\eta(c_m)$	solution viscosity at concentration c_m (kg/m s)
$\eta(0)$	solvent viscosity (kg/m s)

flux resistance through the macroporous structure of the modified membranes.

However, a more speculative reason has been proposed in the literature: the presence of PVP (which is a very hydrophilic polymer) in the membrane could change the hydrophilicity of the membrane, producing a permeability increase [6]. In effect, the >N–C=O group, present in PVP, should interact with the more polar group, O=S=O, present in the PES. The interaction could be of donor/receptor type between >N-C=O and the aromatic ring of PES, as probed by the viscoelastic behaviour of PES–PVP solutions reported by Lafreniere et al. [6] and by Miyano et al. [8]. If the addition of PVP in PES produced only a structural effect, it should not lead to substantial changes in fouling or molecular adsorption on the pore surface of the membrane. Nevertheless, the entrapment of PVP should increase the hydrophilicity and lead to

important changes in the solute filtration and fouling through these membranes.

Actually, the membranes increase their permeability adding PVP with very similar pore size distribution, [11]. This result can be due to three causes:

(a) an increment in the pore density;
(b) a decrease of the effective thickness of the dense layer due to macrovoids in the support layer;
(c) an increment in the hydrophilicity of the surfaces on the membrane and inside the pores.

AFM results show an increment in the surface roughness by PVP addition, and also an increment in the porosity; however, this last result is not decisive. It indicates that, certainly, the structure is modified by the PVP addition. But if the additive remained entrapped, it could also increase the hydrophilicity.In a previous study about the characterization of commercial polysulfone membranes with different pore sizes by XPS and phase contrast AFM [12], a correlation between the nitrogen content on the surface (not present in the polysulfone) and the pore size has been found. The existence of nitrogen, probably due to the addition of PVP during the manufacture of these membranes, shows that PVP could remain on the membrane surface.

In this work, we show the modification of the chemistry of the membrane surface by studying the fouling kinetic of bovine serum albumin (BSA) and DL-histidine (DLH) solutions filtered through the modified membranes, for different PVP contents. The results are analyzed in terms of their hydrophilicity, sizes and electrostatic solute–membrane interactions for pH 4.9. The study is completed with the comparative analysis of the pore size distributions by the retention method of polydisperse solutes in the membranes before and after the fouling process.

2. Theory

2.1. Apparent and true retention

Actually, due to concentration-polarization, a true retention coefficient needs to be defined in terms of the concentration directly in contact with the membrane, $c_m > c_0$ (feed), and the permeate concentration, c_p, as $R = (1 - c_p)/c_m$. The observed retention coefficient, $R_o = (1 - c_p)/c_0$, can be evaluated for different low-pressure drops and thus extrapolated to a zero pressure. Under these extrapolated conditions, the membrane concentration should be very similar to the feed one and thus the so evaluated retention should refer to the membrane itself (true retention) [13].

In order to evaluate the pore size distributions of a partially retaining membrane, it can be assumed that the retention is due to a sieving mechanism. In such a way that for each molecular weight there is a fraction of totally retaining pores, while the rest of them allow a free pass of the molecules [14]. Then, we can write the mass balance for each molecular weight as follows:

$$J_V c_p = J_{V,t} c_m \tag{1}$$

where J_V is the total volumetric flux and $J_{V,t}$ the volumetric flux transmitted through the non-rejection fraction of pores. On the other hand, the ratio of the transmitted volumetric flux and pure water flux, $J_{w,t}$, passing through the transmitting pores is:

$$\frac{J_{V,t}}{J_{w,t}} = \frac{\eta(c_m)}{\eta(0)} \tag{2}$$

where $\eta(c_m)$ and $\eta(0)$ are the solution and solvent viscosities. But, for low c_m this ratio can be approximated to 1 in such a way that Eq. (1) can be rewritten as [15],

$$\left.\begin{aligned} J_{w,t} &= J_V(1 - R) \\ J_{w,r} &= J_V R \end{aligned}\right\} \tag{3}$$

Therefore, $J_{w,t}$ and $J_{w,r}$ (pure water flux passing through the retentive pores) can be evaluated once J_V for each R is known. Then, by again using the mass balance,

$$\left.\begin{aligned} J_V c_p &= J_s \\ J_V - J_s &= J_w \end{aligned}\right\} \tag{4}$$

where c_p has to be expressed as a volume fraction, J_s is the solute flow and J_w is the total pure water flow that can be obtained by this equation. Thus, $J_{w,t}/J_w$ versus the molecular weight gives the accumulated fraction of flux passing through the non-rejecting pores. The derivative of this function should thus provide the flux carrying molecules of a given molecular weight. In order to increase definition an analytical function can be used to interpolate the $J_{w,t}/J_w$ versus the molecular weight M_w. The derivative of this function can easily be calculated point-by-point. To reproduce well

the experimental data, a logical curve, with horizontal asymptotes at $J_{w,t}/J_w = 1$ and 0, seems appropriated:

$$\frac{J_{w,t}}{J_w} = \frac{1}{1 + (M_w/B)^C} \tag{5}$$

where B and C are the constants to be evaluated by fitting Eq. (5) to the experimental results. In this way, $d(J_{w,t}/J_w)/dM_w$ can be obtained. Singh et al. [16], use a lognormal distribution to fit these data; nevertheless, the procedure used by us seems to be more adaptable.

On the other hand, the abscissas can be changed from M_w to pore sizes, d_p, by considering the gyration radii of the PEGs used here as can be obtained from literature [17–20], and fitted to $d_p = (1550 \pm 60) \times 10^{-13} \times M_w^{1/2}$. These resulting pore sizes could be modified by taking into account the number of adsorption layers onto the pore walls and the molecular ability to pass through a pore, from complete rigidity to some degree of flexibility that should allow a size reduction when crossing the membrane [21]. Thus, these assumptions lead to an evaluation of $d(J_{w,t}/J_w)/d(d_p)$.

Finally, the differential flux fraction can be correlated with the pore fraction through the Hagen Poiseuille equation, in such a way that:

$$\frac{d(N/N_T)}{d(d_p)} = \frac{d(J_{w,t}/J_w)}{d(d_p)} \frac{K}{d_p^4} \tag{6}$$

where K is a normalization constant.

For a polydisperse solute, a different retention must be used for each molecular weight that can be defined as follows [11]:

$$R[M_w(i)] = 1 - \frac{\sum_{k=0}^{i} c_{p,k}}{\sum_{k=0}^{i} c_{m,k}} \tag{7}$$

where $\sum_{k=0}^{i} c_{p,k}$ is the solute concentration of the permeate, due to molecules with molecular weights equal or smaller than the i-th one. The concentration $\sum_{k=0}^{i} c_{m,k}$ refers to the solution on the membrane.

2.2. Models of blocking

Blocking filtration mechanisms were first studied by Hermans and Bredée [22]. Gonsalves [23], made a critical study of the physical models used to derive these laws. Grace [24], made a through analysis of the blocking mechanisms in relation to the performance of the filter media to be used, with particular reference to the "standard blocking" process. Finally, Hermia [25], revised all the blocking mechanisms and reformulated the all the mechanisms in a common frame of power-law non-Newtonian fluids.

Attending to the physical causes of these blocking mechanisms, posterior practice has given them more descriptive names that can be used alternatively to the original ones: pore plugging (complete blocking), direct adsorption on the pore walls (standard blocking) and boundary layer resistance (cake filtration).

In any case, the volume flow (m/s) versus time dependency for the complete blocking model should be given by:

$$J_V(t) = J_{V0}\, e^{-K_{CB}t} \tag{8}$$

where

$$K_{CB} = C_{CB} A \frac{\Delta p \pi r_0^4}{8\eta \ell_0} \tag{9}$$

where C_{CB} is the number of pores per surface unit blocked per unit of filtered volume, A the membrane area, η the solution viscosity, Δp the applied pressure, ℓ_0 the membrane thickness and r_0 the initial mean pore size. The Hagen Poiseuille equation has been assumed.

While the rest of the models can be summarised in [3], as follows:

$$J_V(t) = \frac{1}{A}\frac{dV}{dt} = J_{V0}(1 + Kt)^{-n} \tag{10}$$

where for:

- Standard blocking, n is 2 and $K = (1/2)K_S J_{V0}$, where

$$K_S = C_S \frac{A}{2} \left(\frac{J_{V0} \Delta p N_0}{2\eta\pi \ell_0^3} \right)^{1/2} \tag{11}$$

where C_S is the volume deposited on the pore walls per unit of permeated volume and N_0 the initial number of pores per surface unit.

By integrating Eq. (10), we get

$$\frac{t}{V^*} = K_S t + \frac{1}{J_{V0}} \tag{12}$$

with $V^* = V/A$.

- Cake model with $n = 1/2$ and

$$K \equiv 2K_{CF}J_{V0}^2 \tag{13}$$

with

$$K_{CF} = C_{CF}\frac{\rho_C \eta}{\Delta p} \tag{14}$$

where ρ_C is the cake mass per unit of permeated volume and C_{CF} is the apparent specific resistance of the cake. An integration of Eq. (10) leads to,

$$\frac{t}{V^*} = K_{CF}V^* + \frac{1}{J_{V0}} \tag{15}$$

3. Experimental

For each membrane, permeability was first measured followed by the retention experiments of adequate mixtures of PEGs. Another sample from the same batch was instead fouled with BSA or DLH and after rinsing and permeation of bidistilled water during 1 h at 135 kPa, this sample was characterized also by the PEGs retention test.

3.1. Membranes

PES (Ultrason E 6020P, $M_w = 58{,}000$ Da and glass transition temperature $T_g = 225\,^\circ$C) from BASF Aktiengesellschaft, Germany was used. Two kinds of PVP were used: K30 from Fluka ($M_w = 40{,}000$ Da) and K360 from Sigma ($M_w = 360{,}000$ Da). The solvents were *N*,*N*,-dimethylformamide (DMF) and tetrahydrofuran (THF) from Merck (analytical grade).

Three kinds of membranes were laboratory prepared following the standard method of phase inversion technique:

(a) without additive (membrane PES17);
(b) with 2 wt.% PVPK30 (membrane PES17–K30);
(c) with 2 wt.% PVPK360 (membrane PES17–K360).

The PES concentration was 17 wt.% in a casting solution formed by DMF with a 1.5 wt.% of THF.

Casting a polymer solution onto a glass plate made flat membranes. After 30 s of solvent evaporation in ambient atmosphere (20 °C), the membranes were immersed in water (20 °C) for 1 h. Then, the membranes were stored in a glycerine–water solution for 12 h and cleaned with 500 ml water bidistilled prior to be used in the experimental tests.

3.2. Filtration experiments

All filtration experiments have been done in a Minitan-S cell from Millipore. The retentate is circulated on the membrane at a speed of 0.35 m/s controlled by a regulatable peristaltic pump Watson-Marlow 704U/R. The detailed experimental device has been described elsewhere [13].

Besides pure water permeability experiments, the solute retention test has been performed on the studied membranes with 1 g/l solutions (pH = 7) of a mixture of several polyethylene glycols of increasing molecular weights. The solutions were filtered through a membrane area of 3.68×10^{-3} m^2. We used PEGs of analytical grade from Fluka AG. Their molecular weights were 2, 3, 4, 6, 10, 12, 20 and 35 kDa, respectively, with the following proportions: 16.5, 4.6, 5.4, 15.4, 14.3, 3.2, 2.7, and 37.9 wt.%. These proportions give an almost flat molecular weight distribution for the mixtures; i.e. they lead to equal mass concentration for all the molecular weight fractions. True retention was obtained by measuring the observed retention for decreasing pressures (from 135 to 75 kPa) and extrapolating to zero pressure [13].

An HPLC equipment from Shimazdu using also a refractive index detector and provided with a Varian GMPWXL column has been used to obtain the concentration, both for retentate and permeate, for each molecular weight slice, for mixed PEG retention experiments.

3.3. Flux decay

BSA was provided by FLUKA AG, fraction V, no. 05488 with a 98% purity. Its molecular mass is 67000 g/mol with a isoelectric point at pH = 4.9. DLH is an amino acid provided by Sigma catalogue no. H 7750. It has a molecular mass of 155.2 g/mol and an isoelectric point of 7.58. Aqueous solutions of these species with a concentration of 5 g/l at pH = 4.9 have been filtered through the above mentioned membrane system under an applied pressure of 200 kPa during around 2 h. The feed and permeate concentrations have been determined by spectrophotometry at 193 nm for BSA and 202 nm for DLH.

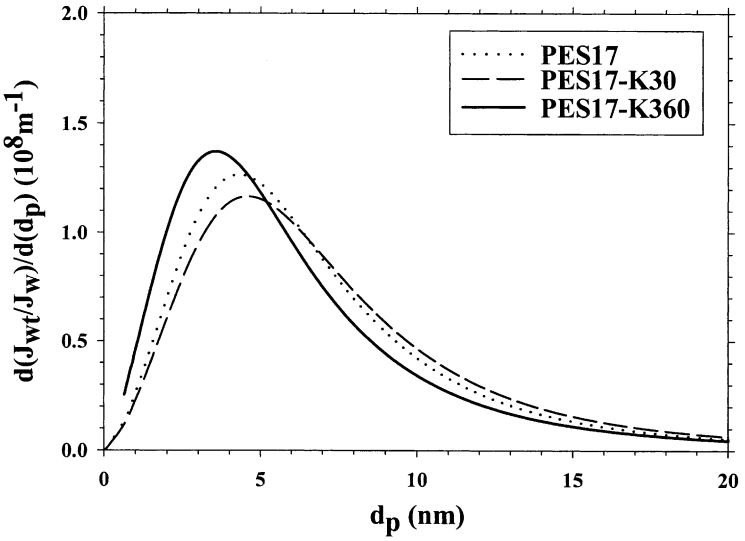

Fig. 1. Normalized differential pore size distribution, attending to flow, obtained by retention experiments [11], for the three membranes studied here. From fittings to lognormals, the following values are obtained: $d_p = 4.06 \pm 0.61$ nm for PES17, $d_p = 4.32 \pm 0.62$ nm for PES17–K30 and $d_p = 3.32 \pm 0.67$ nm for PES17–K360.

4. Results and discussion

In Fig. 1, the normalized differential pore size distribution is shown. The so obtained distributions fit very well to a lognormal leading to $d_p = 4.06 \pm 0.61$ nm for the membrane PES17, $d_p = 4.32 \pm 0.62$ nm for PES17–K30 and $d_p = 3.32 \pm 0.67$ nm for PES17–K360. The error ranges shown correspond to the standard deviations.

4.1. BSA filtration

The molecule of BSA has an elipsoidal equivalent shape with principal axes dimensions of 4.16 nm × 4.16 nm × 14.09 nm which leads to a gyration diameter of 7.28 nm. This means that its size is bigger than the mean pore size (Fig. 1). Actually, retention was very close a 100% in all the cases. Thus, it can be assumed that the resulting fouling should follow mainly external blocking mechanisms, probably starting with a complete blocking first and then a cake fouling.

In Fig. 2, a representation of $\ln J_V$ versus time for the three membranes is shown, this representation should give an straight line when the complete blocking was the more important fouling mechanism acting. It can be seen that this is effectively the case for times below 2000 s. When it is the cake mechanism which is mainly acting, a plot of t/V^* versus V^*, should give a linear fitting as in fact is observed in Fig. 3, for all the cases after values of V^* corresponding to times over 4000 s.

In Table 1, the values for the constants K_{CB} (blocking) and K_{CF} (cake) along with the initial flow, J_{V0}, calculated from Figs. 2 and 3 are shown. The values of the cake and complete blocking constants are directly correlated with the corresponding time constants, K_{CB} and K_{CF} according to Eqs. (9) and (13). In Table 1, the so calculated values for C_{CB}, have been obtained by assuming $\ell_0 = 0.25\,\mu$m, [26], and r_0 according to Fig. 1. Whereas to calculate C_{FC} it has been assumed that the deposited mass per unit of filtered volume, ρ_C, is equal to the feed BSA concentration ($C_{BSA} = 5\,\text{kg/m}^3$). In fact it is strictly true only for dilute concentrations.

The so obtained values for C_{CB} mean that the BSA blocks more pores of the PES17 membrane per unit of filtered volume and membrane area. In particular, 3.33 times those blocked for the PES17–K30 and 1.25 times those blocked for the PES17–K360, respectively.

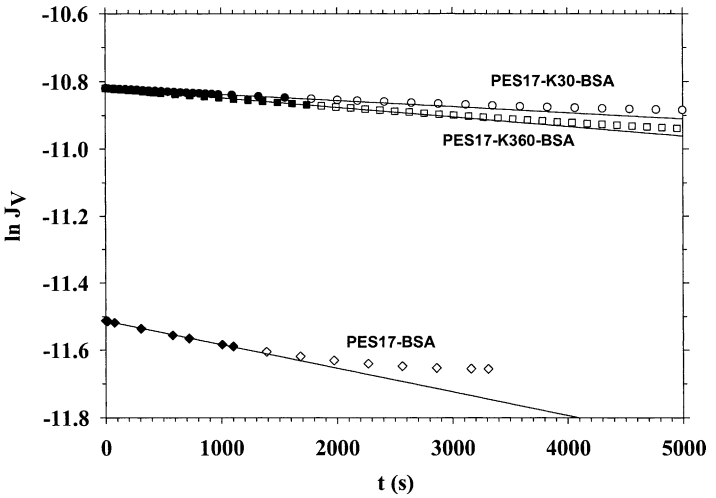

Fig. 2. The $\ln J_V$ for the BSA fouled membranes as a function of time. Straight lines mean good accordance with the complete blocking mechanism.

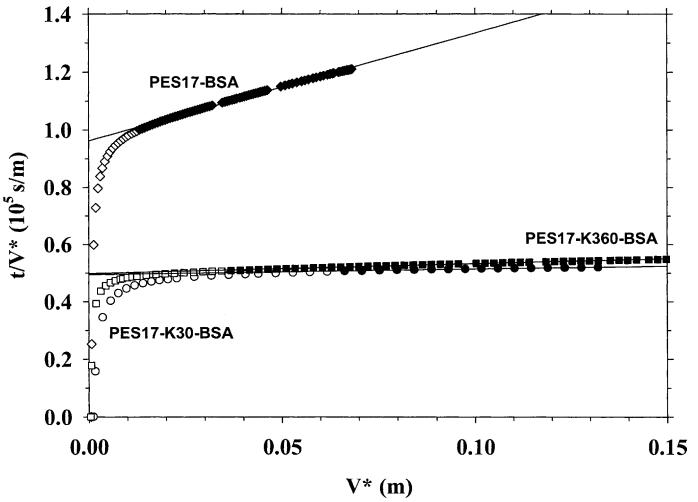

Fig. 3. The t/V^* for the BSA fouled membranes as a function of V^*. Straight lines mean good accordance with the cake fouling mechanism.

Table 1
Values for the fouling mechanisms obtained from Figs. 2 and 3 and Eqs. (9) and (13)

Membrane	J_{V0} ($\times 10^{-5}$ m/s)[a]	Complete blocking			Cake filtration		
		K_{CB} ($\times 10^{-5}$ s^{-1})	C_{CB} ($\times 10^{15}$ m^{-5})	J_{V0} ($\times 10^{-5}$ m/s)	K_{CF} ($\times 10^{5}$ s/m^2)	C_{CF} ($\times 10^{-12}$ m/g)	J_{V0} ($\times 10^{-5}$ m/s)
PES17	1.82	7	11.666	1	7.486	33.942	1.041
PES17–K30	2.05	2	3.499	1.998	0.314	3.237	2.005
PES17–K360	3.113	3	9.340	1.998	0.715	4.602	2.140

[a] Experimental.

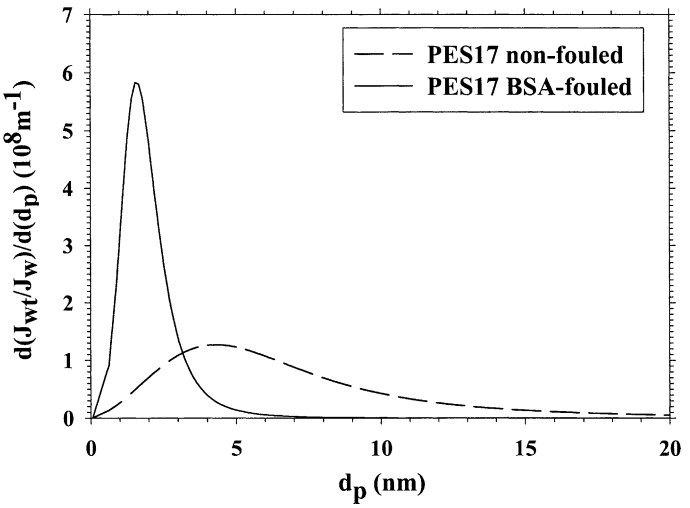

Fig. 4. Normalized differential pore size distribution, attending to flow, obtained by retention experiments for the PES17 membrane after BSA fouling and water rinsing as compared with the corresponding distribution for the non-fouled membrane as shown in Fig. 1.

These results can be explained in terms of the hydrophobic attractive forces between the protein and the membrane that are stronger for the membrane non-containing PVP. BSA is at its isoelectric point thus it is uncharged so, due to the hydrophobic nature of PES it prevents water from disturbing BSA adsorption. Which is not the case for the membranes PVP containing that are more hydrophilic.

Now referring to the cake parameters it is seen that also the apparent specific resistance of the cake is higher for the PES17 than for the other membranes. The cake should be formed by the protein aggregates that effectively are present in the BSA solution at its isoelectric point. The differences between the membrane without and with PVP added should be again due to the higher hydrophobicity of the PES (without PVP) that should lead to a denser first adsorbed layer and thus a tighter packed cake.

Referring to the extrapolated initial flux from both models, they are close within the error range to the experimental ones. These discrepancies can be attributed to the difficulties in dealing with the initial flux measurements when replacing pure water by the feed protein solution.

After BSA ultrafiltration, the PEG retention test was performed by following Eqs. (1)–(7). In Fig. 4, the pore size distribution curve for the PES17 membrane after fouling is compared with that corresponding to the non-fouled membrane. It is clear that for all the membranes the pore size distribution is centered around smaller pore sizes when they have been previously fouled. In Table 2, the corresponding mean diameter and standard deviation for all the BSA fouled and unfouled membranes are shown.

It is clear that these results refer to the fouling that remains under the water rinsing and 1 h permeation through the membranes, in this sense we could say we are characterizing the permanent protein deposition. Thus, this permanent deposition is quite similar for all the membranes leaving opened pores always below 5 nm in diameter (Fig. 4) and average pore reductions from 60 to 70%. The measured permeability reduction, around a 40%, has been also very similar for all the membranes.

Table 2
Average values of d_p, for the three synthesized membranes before and after UF of BSA solutions at pH 4.9

Membrane	$d_p \pm \sigma$ ($\times 10^{-9}$ m)[a]	$d_p \pm \sigma$ ($\times 10^{-9}$ m)[b]
PES17	4.06 ± 0.61	1.58 ± 0.32
PES17–K30	4.32 ± 0.62	1.12 ± 0.45
PES17–K360	3.32 ± 0.67	1.52 ± 0.46

[a] Clean.
[b] Fouled.

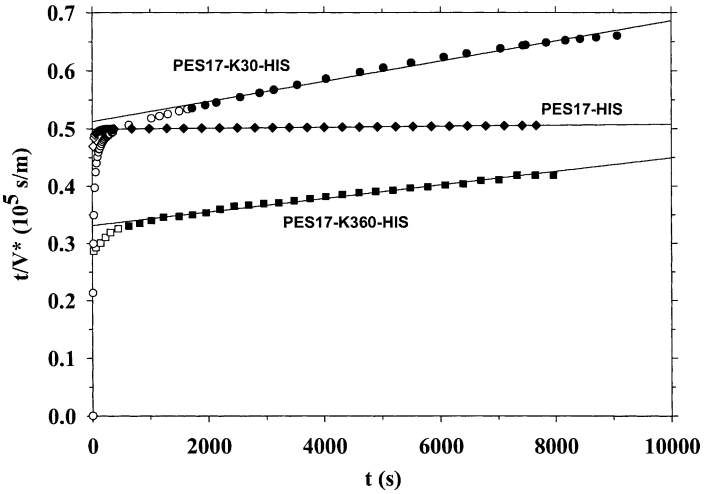

Fig. 5. The t/V^* for the DLH fouled membranes as a function of time. Straight lines mean good accordance with the standard internal fouling mechanism.

4.2. DL-*Histidine filtration*

The much smaller size of DLH as compared with BSA and pore sizes of the membranes as shown in Fig. 1 allow to assume internal fouling instead of external fouling as was the case for the BSA. This fouling occurs almost without rejection (actually less than a 10% retention has been observed in the less favorable conditions) but with a progressive increase in the resistance with time.

Attending to the size relation of DLH and the pores, it seems reasonable to test the standard blocking model. This is also confirmed by the positive second derivative of the resistance versus time [27]. In Fig. 5, t/V^* is shown as a function of time, what should give an straight for the standard blocking model. Results show that there is effectively a linear dependency after a very short (for less 200 s) initial time-span. This initial lack of linearity can be attributed to the stabilization of flux and transmembrane pressure after the introduction of the amino acid solution. The values for the parameters of the standard blocking evaluated for the linear zone are shown in Table 3.

The values of K_S show that the PES17 membrane reduces the effective radii of their pores at a speed 20.5 and 12.2 times slower than PES17–K30 and PES17–K360, respectively. This should be due, again, to the higher hydrophobicity of the non-PVP containing membrane. DLH is positively charged at pH 4.9 (as far as it is below its isoelectric point) thus there is a greater adsorption affinity on the $\succ$N–C=O functional groups present in PVP.

Table 3
Values for the parameters of the standard blocking mechanism

Membrane	J_{V0} ($\times 10^{-5}$ m/s)[a]	Standard blocking	
		K_S ($\times 10^2$ m^{-1})	$J_{V,t}$ ($\times 10^{-5}$ m/s)
PES17	1.82	0.406	2.006
PES17–K30	2.05	8.319	1.960
PES17–K360	3.113	4.947	3.122

[a] Experimental.

The pore size distributions for the PES17 membrane, fouled and unfouled with DLH, are shown in Fig. 6. As for the BSA fouled membranes, they seem to have a lower average pore size. In Table 4, the

Table 4
Average values of d_p, for the three synthesized membranes before and after UF of DLH solutions at pH 4.9

Membrane	$d_p \pm \sigma$ ($\times 10^{-9}$ m)[a]	$d_p \pm \sigma$ ($\times 10^{-9}$ m)[b]
PES17	4.06 ± 0.61	1.57 ± 0.41
PES17–K30	4.32 ± 0.62	1.31 ± 0.35
PES17–K360	3.32 ± 0.67	1.13 ± 0.45

[a] Clean.
[b] Fouled.

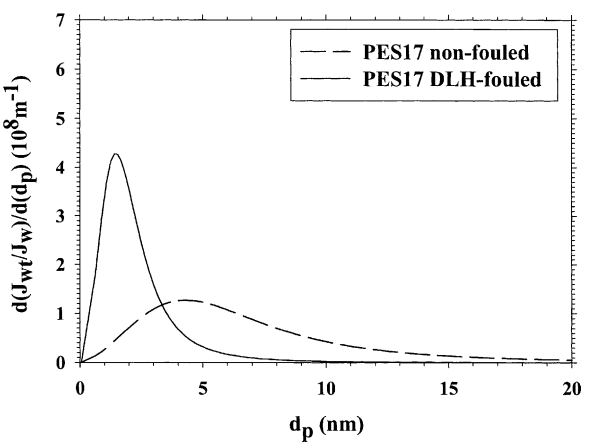

Fig. 6. Normalized differential pore size distribution, attending to flow, obtained by retention experiments for the PES17 membrane after DLH fouling and water rinsing as compared with the corresponding distribution for the non-fouled membrane as shown in Fig. 1.

corresponding mean diameters and standard deviations are shown for all the studied membranes.

As mentioned, these results refer to the fouling that remains under the water cleaning of the membranes. Thus it seems clear that this permanent amino acid deposition is quite similar, both from the pore size distribution and the experimental permeability points of view, for all the membranes and substantially equal when the membranes are fouled by BSA and DLH.

In this case, it is worth noting that the experimental permeability after the pure water treatment is even smaller than the final permeability during the fouling process. This seems to mean that with DLH the water treatment is in fact increasing somehow fouling.

5. Conclusions

Results on BSA fouling seem to indicate that the protein aggregates are initially deposited and block some of the pores afterwards acting as nucleation sites to an increasing cake on the membrane surface. The presence of PVP acts preventing to some extent pore blockage due to its hydrophilic action. This increased hydrophilicity is also preventing the cake from excessive compaction. The more hydrophilic character of the PVP containing membrane along with the positive character of DLH at the used pH causes its faster internal fouling.

The differences in the fouling mechanism can be attributed to the relative sizes of the permeate and the pores of the membrane: giving retention and external fouling when the permeate or its aggregates are clearly over the pore size of the membrane and no significant retention and internal fouling otherwise.

The permanent fouling, that remains after water rinsing and 1 h permeation, is shown to be independent of the presence of PVP added. This is probably due to the elimination of only the cake layer with a remaining similar blocked fraction of pores that water rinsing and permeation is unable to eliminate. Referring to the DLH results, they show that the pore size distributions are also quite similar for all the membranes and to those obtained with BSA. In fact, the cleaning mechanism leads to a, probably only partial, remotion of the adsorbed DLH inside the pores but it also takes pH to its isoelectric point. This should probably lead to aggregation (in fact precipitation as far as at neutral pH, DLH is not soluble in water) inside the pores that should then result in a partial plugging of them, with a similar action to complete blocking. This process could explain the reduction of permeability after the water rinsing and permeation for the membrane fouled with DLH as compared with the final one reached during fouling experiments.

Acknowledgements

The Spanish authors would like to acknowledge the financial support of this work through projects of the “Plan Nacional de Investigación y Desarrollo” MAT1999-0989 and VA62-00B of the Junta de Castilla y León. The Argentine authors would like acknowledge the financial support of this work to “FONCYT (Agencia Nacional de Promoción Cintífica y Tecnológica)”.

References

[1] M. Cheryan, Ultafiltration Handbook, Technomic, Lancaster, UK, 1986.
[2] K.J. Kim, A.G. Fane, C.J.D. Fell, D.C. Joy, Fouling mechanisms of membranes during protein ultrafiltration, J. Membr. Sci. 68 (1992) 79.

[3] C. Herrero, P. Prádanos, J.I. Calvo, F. Tejerina, A. Hernández, Flux decline in protein microfiltration: influence of operative parameters, J. Colloid Interf. Sci. 187 (1997) 344.
[4] I. Cabasso, E. Klein, J.K. Smith, Polysulfone hollow fibers. I. Spinning and properties, J. Appl. Polym. Sci. 20 (1976) 2377.
[5] I. Cabasso, E. Klein, J.K. Smith, Polysulfone hollow fibers. II. Morphology, J. Appl. Polym. Sci. 21 (1977) 165.
[6] L.Y. Lafreniere, F. Talbot, T. Matsuura, S. Sourirajan, Effect of polyvinyl-pyrrolidone additive on the performance of polyethersulfone ultrafiltration membranes, Ind. Eng. Chem. Res. 26 (1987) 2385.
[7] M.R. Torres, E. Soriano, J. de Abajo, J. de la Campa, Comparative study of the behaviour of experimental polyamide UF membranes. The effect of polyvinyl-pyrrolidone used as an additive, J. Membr. Sci. 81 (1993) 31.
[8] T. Miyano, T. Matsuura, S. Sourirajan, Effect of the polyvinyl-pyrrolidone additive on the pore size and the pore size distribution, Chem. Eng. Commun. 119 (1993) 23.
[9] R.M. Boom, T. van den Boomgaard, C.A. Smolders, Mass transfer and thermodynamics during immersion precipitation for a two-polymer system, evaluation with the system PES–PVP–NMO–water, J. Membr. Sci. 90 (1994) 231.
[10] R.M. Boom, Membrane formation by immersion precipitation: the role of a polymeric additive, Ph.D. Thesis, University of Twente, The Netherlands, 1992.
[11] N.A. Ochoa, P. Prádanos, L. Palacio, C. Pagliero, J. Marchese, A. Hernández, Pore size distributions based on AFM imaging and retention of multi-disperse polymers solutes. Characterization of polysulfone UF membranes with dopes containing different PVP, J. Membr. Sci. 187 (2001) 227.
[12] L. Palacio, P. Prádanos, A. Hernández, M.J. Ariza, J. Benavente, M. Nyström, Phase-contrast scanning force microscopy and chemical heterogeneity of GR polysulfone ultrafiltration membranes, Appl. Phys. A 73 (2001) 555–560.
[13] P. Prádanos, J.I. Arribas, A. Hernández, Mass transfer coefficient and retention of PEGs in low pressure cross flow ultrafiltration through asymmetric membranes, J. Membr. Sci. 99 (1995) 1.
[14] M.S. Le, J.A. Howell, Alternative model for ultrafiltration, Chem. Eng. Res. Design 62 (1984) 373.
[15] R. Nobrega, H. de Balmann, P. Aimar, V. Sánchez, Transfer of dextran through ultrafiltration membranes: a study of rejection data analyzed by gel permeation chromatography, J. Membr. Sci. 45 (1989) 17.
[16] S. Singh, K.C. Khulbe, T. Matsuura, P. Ramamurthy, Membrane characterization by solute transport and atomic force microscopy, J. Membr. Sci. 142 (1998) 111.
[17] M. Bodzek, K. Konieczny, The influence of macromolecular mass of polyvinylchloride on the structure and transport characteristics of ultrafiltration membranes, J. Membr. Sci. 61 (1991) 131.
[18] D.R. Lu, S.J. Lee, K. Park, Calculation of solvatation interaction energies for protein adsorption on polymer surfaces, J. Biomater. Sci. Polym. End. 3 (1991) 127.
[19] S. Nakatsuka, A.S. Michaels, Transport and separation of proteins by ultrafiltration through sorptive and non-sorptive membranes, J. Membr. Sci. 69 (1992) 189.
[20] M.N. Sarbolouki, A general diagram for estimating pore size of ultrafiltration and reverse osmosis membranes, Sep. Sci. Tech. 17 (1982) 381.
[21] A. Bessieres, M. Meireles, R. Coratger, J. Beauvillain, V. Sánchez, Investigation of surface properties of polymeric membranes by near field microscopy, J. Membr. Sci. 109 (1996) 271.
[22] P.H. Hermans, H.L. Bredée, Zur kenntnis der filtrations-gesetze, Rec. Trav. Chim. del Pays-Bas 54 (1935) 680.
[23] V.E. Gonsalves, A critical investigation on the viscose filtration process, Rec. Trav. Chim. del Pays-Bas 69 (1950) 873.
[24] H.P. Grace, Structure and performance on filter media, AIChE J. 2 (1956) 307.
[25] J. Hermia, Constant pressure blocking filtration laws. Application to power-law non-Newtonian fluids, Trans. I. Chem. E. 60 (1982) 183.
[26] W.R. Bowen, Q. Gan, Properties of microfiltration membranes: the effects of adsorption and shear on the recovery of an enzyme, Biotechnol. Bioeng. 40 (1992) 491.
[27] E.M. Tracey, R.H. Davis, BSA fouling of track-etched polycarbonate microfiltration membranes, J. Colloid Interf. Sci. 167 (1994) 104.